

Quartic form of the slowly decaying imaginary distance beam propagation method

Hong Shu

College of Optics and Photonics, Center for Research and Education in Optics and Lasers
and Florida Photonics Center of Excellence, University of Central Florida,
Orlando, Florida 32816, USA,
hshu@creol.ucf.edu

Received 28 April 2009; revised 18 June 2009; accepted 22 June 2009;
posted 23 June 2009 (Doc. ID 110696); published 10 July 2009

The governing equation of the slowly decaying imaginary distance beam propagation method (SD-ID-BPM) is further modified, for calculating the eigenmodes in optical fibers and waveguides. Its convergence is analyzed in detail and compared to the earlier version of SD-ID-BPM and other methods. It is demonstrated that the method described here can converge to the same desired accuracy within fewer propagation steps than the earlier version of SD-ID-BPM and other methods. Since the governing equation of the SD-ID-BPM is a partial differential equation with higher order derivatives, it might be interesting if the discretization in the transverse x - y plane is performed by applying the numerical techniques for partial differential equations with higher order derivatives. © 2009 Optical Society of America
OCIS codes: 000.3860, 000.4430, 230.7370.

1. Introduction

There are different types of methods for calculating the eigenmodes in optical guided wave devices [1–10]. The conventional imaginary distance beam propagation method [2,3] has a counterpart in quantum mechanics, which is referred to as “imaginary time” method [11–14]. In [9] the slowly decaying imaginary distance beam propagation method (SD-ID-BPM) is proposed and presented, which is greatly improved in [10] in numerical calculation. In this paper, the governing equation of the SD-ID-BPM is further modified into a quartic form. Using this new method, even fewer propagation steps are needed to reach the same desired accuracy compared to the earlier version of SD-ID-BPM [10] and other methods. Detailed analysis and comparison will be performed on this method. To demonstrate the method, the scalar formulation is used, and it is straightforward to extend it to vector formulation. As a convenient way for demonstration of the method, the finite difference method was used for the discre-

tization in the x - y plane. Other methods including the finite element method (variational or discontinuous Galerkin) [15–21] and the pseudospectral method [22,23] may be suitable for discretization in the transverse x - y plane.

2. Formulation and Analysis

The governing equation of the SD-ID-BPM is [9,10]

$$\frac{\partial A}{\partial z} = -j \cdot \frac{(H - \alpha) \cdot (\alpha - H)}{c} \cdot A \quad (1)$$

if scalar formulation is used, where

$$H = \frac{1}{2k_0 n_0} \cdot \left[\frac{\partial^2}{\partial x^2} + \frac{\partial^2}{\partial y^2} + k_0^2 \cdot (n^2 - n_0^2) \right] \quad (2)$$

if the guiding is weak, such as that in a weakly guiding step index fiber. k_0 is the vacuum wave number, n_0 is the reference refractive index, and n is the refractive index in the considered guiding structures. Here only real n will be considered. n , and hence H , are invariant along the imaginary z axis. For a waveguide structure that varies along the longitudinal

direction (note that this is not the imaginary z axis in SD-ID-BPM), n in Eq. (2) represents the transverse index distribution at a specific position along the longitudinal direction in the considered waveguide, where the eigenmodes are of interest.

It can be seen that Eq. (1) is quadratic in H . Here a governing equation that is quartic in H is proposed, which is

$$\frac{\partial A}{\partial z} = j \cdot \frac{(H - \alpha)^4}{\delta} \cdot A, \quad (3)$$

where $z = j \cdot z'$ and z' is real. Similar to [9] and [10], α is a constant with the dimension of m^{-1} . δ is a constant with the dimension of m^{-3} . H is still as defined in Eq. (2).

Both the governing equation of the quadratic SD-ID-BPM [9,10] and the governing equation of the quartic SD-ID-BPM described here are typical higher order partial differential equations, in which there are higher order spatial derivatives. In Eq. (3) the differential operator $(H - \alpha)^4$ can be expanded and an equivalent differential operator can be obtained, in which the highest order spatial derivative is eight. Similarly, the highest order spatial derivative in the governing equation of the quadratic SD-ID-BPM [9,10] is four.

First the formal solution of Eq. (3) is considered. Since H is z invariant, the formal solution of Eq. (3) can be written as

$$A(x, y, z) = e^{j \frac{(H - \alpha)^4}{\delta} z} \cdot A(x, y, z = 0). \quad (4)$$

Any arbitrary input can be expanded in the complete set of the eigenfunctions of the operator H , as

$$A(x, y, 0) = \sum_m a_m \phi_m(x, y), \quad (5)$$

with

$$H \cdot \phi_m(x, y) = \lambda_m \phi_m(x, y), \quad (6)$$

where $\phi_m(x, y)$ is the eigenfunction for the m th eigenmode, and the corresponding eigenvalue is $\lambda_m = (\beta_m^2 - k_0^2 n_0^2) / (2k_0 n_0)$ [5,7] with β_m representing the propagation constant.

Inserting Eqs. (5) and (6) into Eq. (4) and using $z = j \cdot z'$, the following can be obtained:

$$A(x, y, z') = \sum_m a_m e^{-\frac{(\lambda_m - \alpha)^4}{\delta} z'} \phi_m(x, y). \quad (7)$$

The purpose here is to extract the eigenmodes in optical fibers and waveguides, including the fundamental and all the higher order guided modes. In order to achieve fast convergence to the targeted mode in the numerical calculation, the fully implicit scheme will be used for the discretization of Eq. (3) in the z direction, and this is similar to the choice of the fully implicit scheme in [10]. For the purpose of

analysis the fully implicit scheme is first applied in the z direction without discretization in the x - y plane, and Eq. (3) becomes

$$A(x, y, z' + \Delta z') = \frac{1}{1 + \Delta z' \frac{(H - \alpha)^4}{\delta}} \cdot A(x, y, z'), \quad (8)$$

where H is defined in Eq. (2) since the scalar formulation is used. Again using the complete set of the eigenfunctions of the operator H , both $A(x, y, z' + \Delta z')$ and $A(x, y, z')$ can be expanded as

$$\begin{aligned} A(x, y, z') &= \sum_m a_m(z') \phi_m(x, y), \\ A(x, y, z' + \Delta z') &= \sum_m a_m(z' + \Delta z') \phi_m(x, y). \end{aligned} \quad (9)$$

Applying Eq. (9) to Eq. (8) results in

$$\begin{aligned} \sum_m a_m(z' + \Delta z') \phi_m(x, y) &= \sum_m a_m(z') \frac{1}{1 + \Delta z' \frac{(\lambda_m - \alpha)^4}{\delta}} \\ &\times \phi_m(x, y). \end{aligned} \quad (10)$$

From Eq. (10) the following can be obtained:

$$a_m(z' + \Delta z') = \frac{1}{1 + \Delta z' \frac{(\lambda_m - \alpha)^4}{\delta}} a_m(z'). \quad (11)$$

It can be seen that the modulus of the amplification factor for the m th mode is $|1/[1 + (\Delta z'/\delta)(\lambda_m - \alpha)^4]|$ for each propagation step. Since both $\Delta z'$ and δ are chosen to be positive and real, and α is also chosen to be real, $|1/[1 + (\Delta z'/\delta)(\lambda_m - \alpha)^4]| \leq 1$ is generally valid when analyzing guiding structures with real refractive index. Therefore, the method presented here is numerically stable, and there is no singular point in the amplification factor during the numerical propagation. The analysis on the convergence of the numerical solution using the fully implicit scheme is based on Eq. (11). On the other hand, when $\Delta z'/\delta$ is very large, the difference between Eqs. (7) and (10) is generally very large. However, in the context of eigenmode calculation, large $\Delta z'/\delta$ is preferred for fast convergence of the numerical calculation using the fully implicit scheme in the z direction, even though it is very different from the formal solution of the governing equation. This is essentially the same as the discussion presented in [10]. The purpose here is to extract an eigenmode; the conservation of energy does not need to be obeyed, and the governing equation itself does not correspond to any physical system that exists in the real world. Both SD-ID-BPM (quadratic and quartic) and the conventional ID-BPM are mathematical methods for calculating the eigenmodes. The propagators for the SD-ID-BPM and the conventional ID-BPM are not unitary, just like the propagator for the imaginary time formalism of the Schrodinger equation [11].

In the practical numerical solution, Eq. (8) needs to be further discretized in the x - y plane. No matter what type of discretization is used in the x - y plane, such as the finite difference method, the finite element method [15–21], or other methods, including the pseudospectral method [22,23], the analysis presented here is valid.

Shown in Fig. 1 is the plot of the modulus of the amplification factor in Eq. (11), as a function of $b = (\Delta z'/\delta)(\lambda_m - \alpha)^4$. The monotonicity guarantees that the mode with the eigenvalue that is the closest to the chosen α has the largest modulus of the amplification factor. The quartic SD-ID-BPM maintains all the advantages of the quadratic SD-ID-BPM presented in [10] (summarized right before the conclusion section there), and it will be demonstrated that the number of propagation steps needed to reach a specific accuracy using the quartic SD-ID-BPM is fewer than that using the quadratic SD-ID-BPM.

3. Numerical Results and Discussions

For demonstration the common finite difference method [24–26] was used for the discretization of the differential operator $(H - \alpha)$ in Eq. (8) in the x - y plane. Similar to the calculation described in [9] and [10], the differential operator $(H - \alpha)$ was first discretized, and the common finite difference method described in [24–26] was used. As a result, the discretized version of Eq. (8) can then be written as

$$A^{l+1} = \frac{I}{I + \Delta z' \frac{(H^{(n)} - \alpha I)^4}{\delta}} \cdot A^l, \quad (12)$$

where $H^{(n)}$ is the discretized version of H and is a sparse matrix, A^{l+1} and A^l are the discretized versions of A and are vectors, I is an identity matrix with the same dimension as $H^{(n)}$, and the superscript l represents the index of the discrete z coordinate.

Note that the discretization in the x - y plane used for obtaining Eq. (12) is only a convenient way for

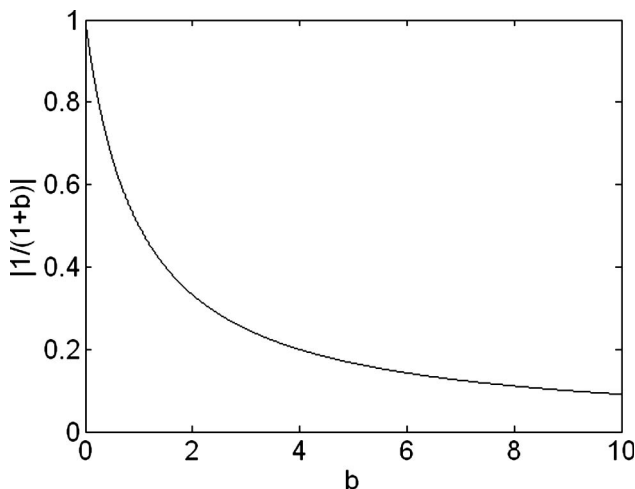


Fig. 1. Plot of the modulus of the amplification factor as a function of $b = (\Delta z'/\delta)(\lambda_m - \alpha)^4$.

demonstration of the method, and the number of nonzero matrix elements in the sparse matrix $(H^{(n)} - \alpha I)^4$ could be more than that in $(H^{(n)} - \alpha I)$. A possibly better way for discretization is to first expand the fourth order term for the differential operator $(H - \alpha)^4$ in Eq. (3), to obtain an equivalent differential operator that contains eighth order differentiations with respect to x and y , and so on. After the expansion of the differential operator $(H - \alpha)^4$ the discretization can then be conducted in the x - y plane for numerical solution. The methods other than the finite difference method, including the finite element method (using the variational principle or the discontinuous Galerkin method) [15–21], and possibly other methods including the pseudospectral method [22,23], might be suitable for discretization in the x - y plane. In the z direction the fully implicit scheme shall be used.

According to Eq. (11), after the solution converges well to the dominant mode, its eigenvalue can be calculated according to

$$\lambda_i = \alpha \pm \left\{ \left[\frac{A(x_0, y_0, z')}{A(x_0, y_0, z' + \Delta z')} - 1 \right] \cdot \frac{\delta}{\Delta z'} \right\}^{\frac{1}{4}}, \quad (13)$$

where x_0 and y_0 are the coordinates for some specific point in the transverse plane. Generally speaking, x_0 and y_0 can be chosen so that the modulus of the field amplitude at this point is not zero and preferably not too small. The propagation constant of the dominant mode is then $\beta_i = k_0 n_0 \cdot \sqrt{1 + 2 \lambda_i / (k_0 n_0)}$ [10].

For demonstration the same weakly guiding step index fiber used for the calculation in [10] is considered here. The core index $n_{\text{core}} = 1.469$, the index in the cladding $n_{\text{clad}} = 1.46$, the laser wavelength is $1.03 \mu\text{m}$, and the diameter of the fiber core is $10.1 \mu\text{m}$. A square transverse computation window was used with $w_x = w_y = 35 \mu\text{m}$, the transverse step sizes $\Delta x = \Delta y \cong 0.292 \mu\text{m}$. The step size in the z' axis was fixed at $\Delta z' = 10 \mu\text{m}$. The reference index was fixed at $n_0 = (n_{\text{core}} + n_{\text{clad}})/2$ for all the calculations in this paper. The zero value boundary conditions were used in the calculation. The input of the calculation was a summation of many different functions of x and y , so that the input may include as many modes as possible.

Again, the MATLAB function “bicgstab” using the biconjugate gradients stabilized method (BICGSTAB) [27] was not used for solving the sparse matrix equation, for the same reason as described in [10]. Instead the Gaussian elimination (LU factorization) in MATLAB was used for solving the sparse matrix equation.

Shown in Fig. 2 are the plots of the number of propagation steps needed to converge to a specific accuracy (effective index converges to within 10^{-5} from the eventual solution), as a function of the parameter δ . From Fig. 2 it can be seen that, so long as δ is small enough at fixed $\Delta z'$, the effective index of the targeted mode can reach the desired accuracy in only two propagation steps. This is true for all the other

guided modes too, in addition to the LP₀₁ and LP₀₂ modes shown in Fig. 2.

Shown in Fig. 3 are the plots of the convergence of β_-/k_0 (β_+/k_0 is not the right solution of the effective index), for the LP₀₁ mode as a function of the propagation step number. In the calculation for Fig. 3, $\alpha = (k_0^2 n_{\text{core}}^2 - k_0^2 n_0^2)/(2k_0 n_0)$ and $\delta = 10^8 \text{ m}^{-3}$. For comparison the calculation using the quadratic SD-ID-BPM [10] is also plotted in Fig. 3 with the same α and $c = 10^{-2} \text{ m}^{-1}$. The same input as that used in [10] was used here for the calculations using both the quartic and quadratic SD-ID-BPM, which is basically a summation of many different functions of x and y , so that the input may include as many modes as possible. This same input was also used for all the

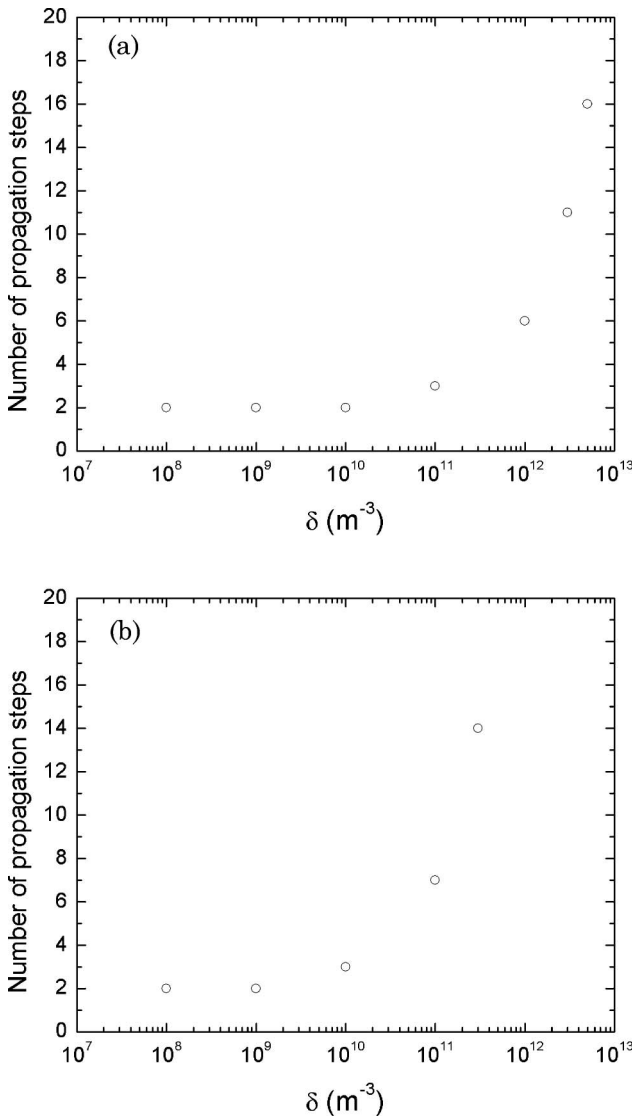


Fig. 2. Plot of the number of propagation steps needed to converge to a specific accuracy as a function of the parameter δ for the considered step index fiber. The specific accuracy is for the effective index converging to within 10^{-5} from the eventual solution. (a) LP₀₁ mode with α set to be $\alpha = (k_0^2 n_{\text{core}}^2 - k_0^2 n_0^2)/(2k_0 n_0)$. (b) LP₀₂ mode with α set to be $\alpha = (k_0^2 \cdot 1.4615^2 - k_0^2 n_0^2)/(2k_0 n_0)$.

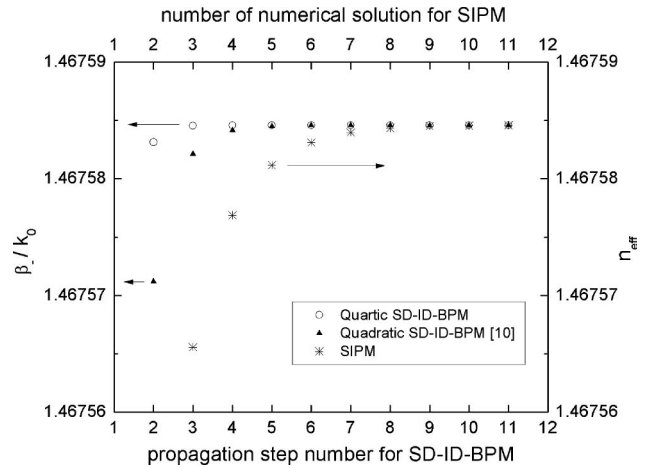


Fig. 3. Plots of the convergence of β_-/k_0 for the LP₀₁ mode as a function of the propagation step number for the considered step index fiber, with α set to be $\alpha = (k_0^2 n_{\text{core}}^2 - k_0^2 n_0^2)/(2k_0 n_0)$. The open circles represent the calculation using the quartic SD-ID-BPM with $\delta = 10^8 \text{ m}^{-3}$; the solid triangles represent the calculation using the quadratic SD-ID-BPM [10] with $c = 10^{-2} \text{ m}^{-1}$. The stars represent the convergence of the calculated effective index n_{eff} as a function of number of numerical solutions using Eq. (14), with α set to be $\alpha = (k_0^2 n_{\text{core}}^2 - k_0^2 n_0^2)/(2k_0 n_0)$.

other calculations in this paper including the calculations shown in Fig. 2.

Another quite fast method for eigenmode calculation is the shifted inverse power method (SIPM) [6,23,28–30]. Using the same notation as in Eq. (12), the numerical calculation using the shifted inverse power method can be written as

$$A^{l+1} = \frac{I}{H^{(n)} - \alpha I} A^l. \quad (14)$$

For comparison the convergence of the calculated effective index n_{eff} as a function of the number of numerical solutions using Eq. (14) is also plotted in Fig. 3, using the same $\alpha = (k_0^2 n_{\text{core}}^2 - k_0^2 n_0^2)/(2k_0 n_0)$ and the same input for the calculation.

Shown in Fig. 4 are the plots of the convergence of β_+/k_0 (β_-/k_0 is not the right solution of the effective index) for the LP₀₂ mode as a function of the propagation step number. In the calculation for Fig. 4, $\alpha = (k_0^2 \cdot 1.4615^2 - k_0^2 n_0^2)/(2k_0 n_0)$; for the calculation using the quartic SD-ID-BPM, $\delta = 10^8 \text{ m}^{-3}$, and for the calculation using the quadratic SD-ID-BPM [10], $c = 10^{-2} \text{ m}^{-1}$. The calculation using the shifted inverse power method is also plotted in Fig. 4 for comparison, and the same $\alpha = (k_0^2 \cdot 1.4615^2 - k_0^2 n_0^2)/(2k_0 n_0)$ was used when solving Eq. (14). Again the same input used for the calculations shown in Fig. 3 was used for all the calculations shown in Fig. 4.

From Figs. 3 and 4 it can be seen that the quartic SD-ID-BPM needs the least number of propagation steps to reach the same accuracy compared to the quadratic SD-ID-BPM and the shifted inverse power method. In addition, both the quartic and quadratic SD-ID-BPM need fewer number of propagation steps

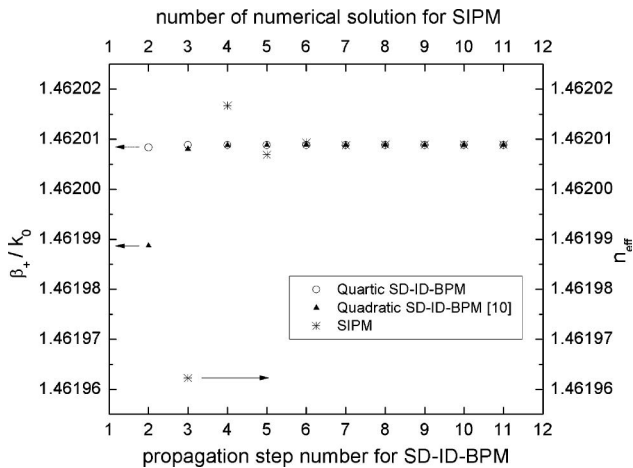


Fig. 4. Plots of the convergence of β_+/k_0 for the LP_{02} mode as a function of the propagation step number for the considered step index fiber, with α set to be $\alpha = (k_0^2 \cdot 1.4615^2 - k_0^2 n_0^2)/(2k_0 n_0)$. The open circles represent the calculation using the quartic SD-ID-BPM with $\delta = 10^8 \text{ m}^{-3}$; the solid triangles represent the calculation using the quadratic SD-ID-BPM [10] with $c = 10^{-2} \text{ m}^{-1}$. The stars represent the convergence of the calculated effective index n_{eff} as a function of number of numerical solutions using Eq. (14), with α set to be $\alpha = (k_0^2 \cdot 1.4615^2 - k_0^2 n_0^2)/(2k_0 n_0)$.

to reach the same accuracy than the shifted inverse power method. The reason for this can be understood by looking at the modulus of the amplification factor for each mode for these methods.

According to the author's knowledge, the number of propagation steps needed to reach the same accuracy is the least using the quartic SD-ID-BPM compared to any other previously existing methods. As discussed above, a possibly better way of discretization is to first expand the fourth order term for the differential operator $(H - \alpha)^4$ in Eq. (3), and to obtain an equivalent differential operator that contains eighth order differentiations with respect to x and y . After the expansion of the differential operator $(H - \alpha)^4$ in Eq. (3), the discretization can then be performed in the x - y plane. On the other hand, the finite element method [15–21], and possibly other methods including the pseudospectral method [22,23], might be suitable for the discretization in the x - y plane in the quartic SD-ID-BPM. Again in the z direction, the fully implicit scheme shall be used.

Another advantage of SD-ID-BPM (both quartic and quadratic) is the good numerical stability. It might be convincing to consider the shifted inverse power method for comparison. The shifted inverse power method is basically ill conditioned just like the imaginary distance beam propagation method described in [5] and [7], since there exist singular points in the amplification factor, although in the practical calculation it is almost impossible to meet a singular point exactly. Although the field can be normalized after each step of the calculation in the practical calculation using the shifted inverse power method, it is hard to control how much the field will be amplified or decayed for each step of the calculation

[the solution of Eq. (14)]. The shifted inverse power method is not a healthy algorithm from the point of view of mathematics. On the other hand, the SD-ID-BPM (both quartic and quadratic) is well conditioned from the point of view of mathematics. In the practical calculation using SD-ID-BPM it is easier to control how much the field will be decayed (it will not be amplified).

Some techniques could be useful in the practical implementation of SD-ID-BPM (both quartic and quadratic). For example, the parameter α can be updated after each propagation step by setting $\alpha = (k_0^2 n_{\text{new}}^2 - k_0^2 n_0^2)/(2k_0 n_0)$, where n_{new} is the effective index newly updated after each propagation step. Since n_{new} will get closer and closer to the effective index of the targeted mode, the modulus of the amplification factor will get closer and closer to one for both quartic and quadratic SD-ID-BPM. When the chosen α is close to the eigenvalue of the targeted mode, the decay of the targeted mode is very slow, while all the other modes decay very quickly, which is why this method is referred to as “slowly decaying ID-BPM.”

Finally, the quartic form of SD-ID-BPM can be further extended to a sixth order or even higher order form if it is necessary, and the governing equation can be written as

$$\frac{\partial A}{\partial z} = j \cdot \frac{(H - \alpha)^{2N}}{S^{2N-1}} \cdot A, \quad (15)$$

where $z = j \cdot z'$ and z' is real, α is a constant with the dimension of m^{-1} , S is a constant with the dimension of m^{-1} , H is still as defined in Eq. (2) if scalar formulation is used, and N is a positive integer. When $N = 1$, Eq. (15) is the governing equation of the quadratic SD-ID-BPM [9,10]. When $N = 2$, Eq. (15) is the governing equation of the quartic SD-ID-BPM.

In many practical cases the waveguide structures vary in the propagation direction although the variation is generally slow on the scale of the considered laser wavelength [31]. In these cases the eigenmodes calculated by the SD-ID-BPM are the local eigenmodes at a specific position along the propagation direction, if the transverse index distribution for this specific position along the propagation direction is used to define the H operator according to Eq. (2).

4. Conclusion

A quartic form of the slowly decaying imaginary distance beam propagation method is presented. The governing equation has been modified. Using the finite difference method in the transverse x - y plane it has been demonstrated that, to reach the same accuracy, the number of propagation steps needed is fewer using the quartic SD-ID-BPM than that using the quadratic SD-ID-BPM and the shifted inverse power method. In addition, the finite difference method is probably not the best choice for the discretization in the x - y plane. Instead, other methods including the finite element method, the

pseudospectral method, or even other methods might be particularly suitable for the discretization in the x - y plane. In the z direction the fully implicit scheme shall be used. In addition, both the quadratic and quartic SD-ID-BPM should be able to be applied to solve the time-independent Schrodinger equation, which is an eigen problem, and it can be referred to as the “slowly decaying imaginary time method.”

References

1. M. D. Feit and J. A. Fleck Jr., “Computation of mode properties in optical fiber waveguides by a propagating beam method,” *Appl. Opt.* **19**, 1154–1164 (1980).
2. D. Yevick and W. Bardyszewski, “Correspondence of variational finite-difference (relaxation) and imaginary-distance propagation methods for modal analysis,” *Opt. Lett.* **17**, 329–330 (1992).
3. C. L. Xu, W. P. Huang, and S. K. Chaudhuri, “Efficient and accurate vector mode calculations by beam propagation method,” *J. Lightwave Technol.* **11**, 1209–1215 (1993).
4. J. C. Chen and S. Jungling, “Computation of higher-order waveguide modes by imaginary-distance beam propagation method,” *Opt. Quantum Electron.* **26**, S199–S205 (1994).
5. S. Jungling and J. C. Chen, “A study and optimization of eigenmode calculations using the imaginary-distance beam-propagation method,” *IEEE J. Quantum Electron.* **30**, 2098–2105 (1994).
6. C. L. Xu, W. P. Huang, M. S. Stern, and S. K. Chaudhuri, “Full-vectorial mode calculations by finite difference method,” *IEE Proc. Optoelectron.* **141**, 281–286 (1994).
7. M. M. Spuhler, D. Wiesmann, P. Freuler, and M. Diergardt, “Direct computation of higher-order propagation modes using the imaginary-distance beam propagation method,” *Opt. Quantum Electron.* **31**, 751–761 (1999).
8. P. Chamorro-Posada, “A modified imaginary distance BPM for directly computing arbitrary vector modes of 3-D optical waveguides,” *J. Lightwave Technol.* **21**, 862–867 (2003).
9. H. Shu and M. Bass, “Calculating the guided modes in optical fibers and waveguides,” *J. Lightwave Technol.* **25**, 2693–2699 (2007).
10. H. Shu and M. Bass, “Analysis and optimization of the numerical calculation in the slowly decaying imaginary distance beam propagation method,” *J. Lightwave Technol.* **26**, 3199–3206 (2008).
11. R. Shankar, *Principles of Quantum Mechanics*, 2nd ed. (Plenum, 1994), Chap. 21.
12. S. V. Lawande, C. A. Jensen, and H. L. Sahlin, “He and $H^{-1}S$ and 2^3S states computed from Feynman path integrals in imaginary time,” *J. Chem. Phys.* **54**, 445–452 (1971).
13. D. Blume, M. Lewerenz, P. Niyaz, and K. B. Whaley, “Excited states by quantum Monte Carlo methods: imaginary time evolution with projection operators,” *Phys. Rev. E* **55**, 3664–3375 (1997).
14. K. E. Schmidt, P. Niyaz, A. Vaught, and M. A. Lee, “Green’s function Monte Carlo method with exact imaginary-time propagation,” *Phys. Rev. E* **71**, 016707 (2005).
15. K. Saitoh and M. Koshiba, “Full-vectorial imaginary-distance beam propagation method based on a finite element scheme: application to photonic crystal fibers,” *IEEE J. Quantum Electron.* **38**, 927–933 (2002).
16. M. Koshiba and Y. Tsuji, “Curvilinear hybrid edge/nodal elements with triangular shape for guided-wave problems,” *J. Lightwave Technol.* **18**, 737–743 (2000).
17. Y. Tsuji and M. Koshiba, “Guided-mode and leaky-mode analysis by imaginary distance beam propagation method based on finite element scheme,” *J. Lightwave Technol.* **18**, 618–623 (2000).
18. S. S. A. Obayya, B. M. A. Rahman, K. T. V. Grattan, and H. A. El-Mikati, “Full vectorial finite-element-based imaginary distance beam propagation solution of complex modes in optical waveguides,” *J. Lightwave Technol.* **20**, 1054–1060 (2002).
19. Y. D. Cheng and C. W. Shu, “A discontinuous Galerkin finite element method for time dependent partial differential equations with higher order derivatives,” *Math. Comput.* **77**, 699–730 (2008).
20. J. Yuan and C. W. Shu, “Local discontinuous Galerkin methods for partial differential equations with higher order derivatives,” *J. Sci. Comput.* **17**, 27–47 (2002).
21. J. Yuan and C. W. Shu, “A local discontinuous Galerkin method for KdV type equations,” *SIAM J. Numer. Anal.* **40**, 769–791 (2002).
22. C. C. Huang, “Simulation of optical waveguides by novel full vectorial pseudospectral-based imaginary distance beam propagation method,” *Opt. Express* **16**, 17915–17934 (2008).
23. P. J. Chiang, C. P. Yu, and H. C. Chang, “Analysis of two-dimensional photonic crystals using a multidomain pseudospectral method,” *Phys. Rev. E* **75**, 026703 (2007).
24. Y. Chung and N. Dagli, “An assessment of finite difference beam propagation method,” *IEEE J. Quantum Electron.* **26**, 1335–1339 (1990).
25. A. Goldberg, H. M. Schey, and J. L. Schwartz, “Computer-generated motion pictures of one-dimensional quantum-mechanical transmission and reflection phenomena,” *Am. J. Phys.* **35**, 177–186 (1967).
26. W. H. Press, B. P. Flannery, S. A. Teukolsky, and W. T. Vetterling, *Numerical Recipes in Pascal* (Cambridge University, 1989).
27. H. A. Van Der Vorst, “BI-CGSTAB: a fast and smoothly converging variant of BI-CG for the solution of nonsymmetric linear systems,” *SIAM J. Sci. Stat. Comput.* **13**, 631–644 (1992).
28. M. S. Stern, “Semivectorial polarized finite difference method for optical waveguides with arbitrary index profiles,” *IEE Proc. J. Optoelectron.* **135**, 56–63 (1988).
29. R. Scarmozzino, A. Gopinath, R. Pregla, and S. Helfert, “Numerical techniques for modeling guided-wave photonic devices,” *IEEE J. Sel. Top. Quantum Electron.* **6**, 150–162 (2000).
30. Y. L. Hsueh, M. C. Yang, and H. C. Chang, “Three-dimensional noniterative full-vectorial beam propagation method based on the alternating direction implicit method,” *J. Lightwave Technol.* **17**, 2389–2397 (1999).
31. Y. Y. Lu, “Some techniques for computing wave propagation in optical waveguides,” *Commun. Comput. Phys.* **1**, 1056–1075 (2006).